Computational studies in actinide chemistry

Free University of Amsterdam

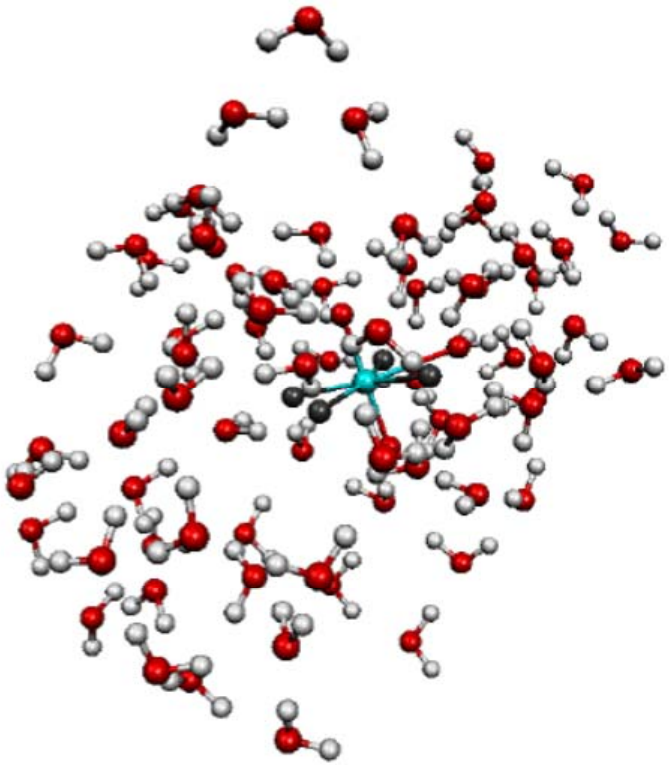

The uranyl fluoride [$UO_2F_4^{2-}$] complex

- Structure optimization using QM/MM & single point full QM calculations for relative energies
- Microscopic model improves on continuum models by explictly including hydrogen bonding
- Feasible for studies of large solvated actinide complexes

I. Infante and L. Visscher, *A QM/MM study of aqueous solvation of the uranyl fluoride [$UO_2F_4^{2-}$] complex,* J. Comp. Chem. (in press).

Actinide-Klaui Complexes

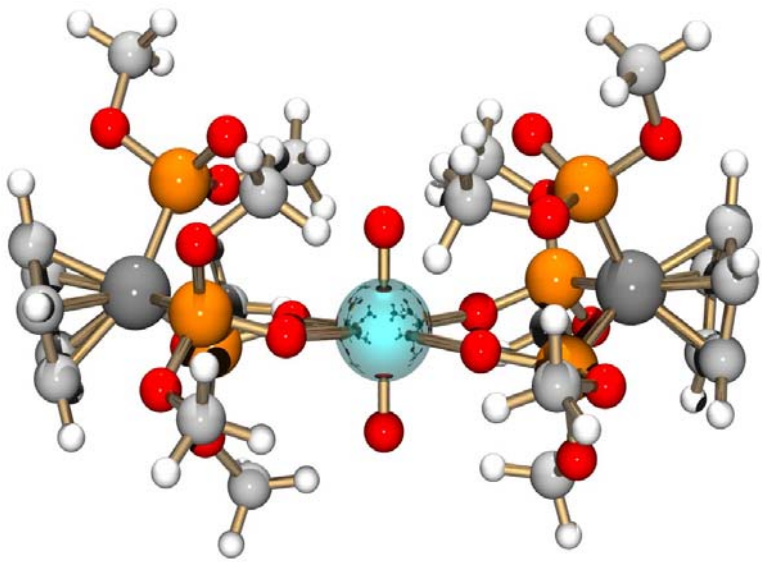

Geometry of UO_2(Kläui)$_2$ sandwich complex

Relativistic density functional theoretical modeling has been carried out on the actinide/lanthanide complexes with the tripodal Kläui ligands $CpCo[OP(OR)_2]_3^-$ to explore the geometries, bonding, and electronic structures of these compounds that have potential applications in actinide separation. We find that

(1) Substitution of the H atoms in the $CpCo[OP(OH)_2]_3^-$ ligand by Me, Et, and Pr groups help to increase the electron donating ability of the Kläui ligands
(2) Geometry optimizations on the (Kläui)$M(H_2O)_x(NO_3)_2$ (M = Th, La; x = 1, 2) complexes indicate that Th and La prefer nine-coordination and eight-coordination, respectively
(3) Due to linearity of the uranyl unit, the Kläui ligands are forced to behavior only as bidentate instead of tridentate chelating agents (see figure on the left)
(4) Kläui ligands can form semi-sandwich or sandwich complexes with La^{3+}, Th^{4+}, U^{4+} and UO_2^{2+}, indicating they have strong ability to coordinate to lanthanide and actinide cations and thus are good binding anions for separating lanthanides from actinides

Ab Initio Study of Extraction Specificity of An^{3+} and Ln^{3+}

CSD/LBNL

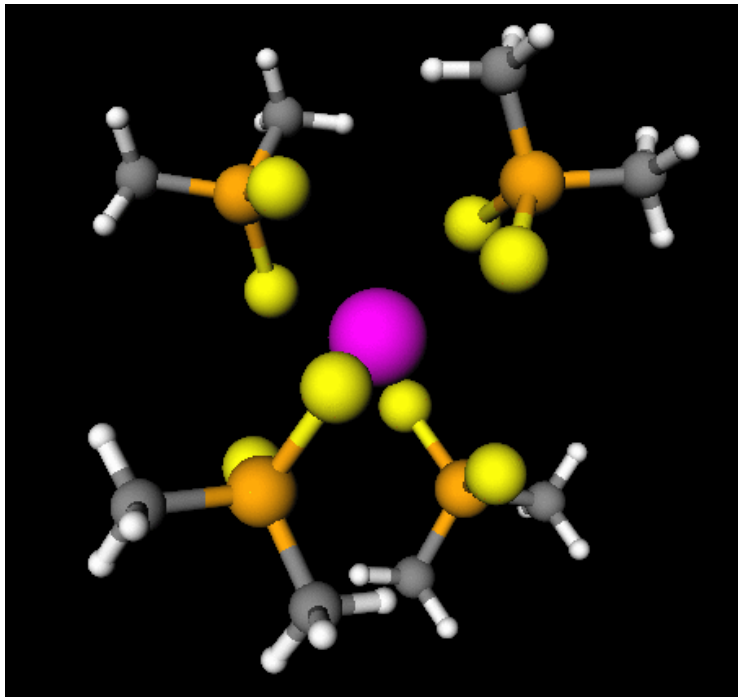

$AmS_2P_2(CH_3)_2^-$ structure

Am(III) and Cm(III) are chemically similar to the Ln(III) elements and thus present a challenge for their separation from the Ln(III) in nuclear wastes.

Organodithiophosphinates have great selectivity for Am(III) over the Ln(III) elements. Experiments show that there is an extra water in the first ligand shell of Ln(III) compared with Am(III). The structural difference is suggested as the basis for the selectivity.

DFT calculations, with spin-orbit effects included, are carried out to understand the basis in the structural differences. Steric and covalent effects are analyzed to explain the structural differences.

Calculation on ^{17}O NMR parameters in uranyl carbonate crystals

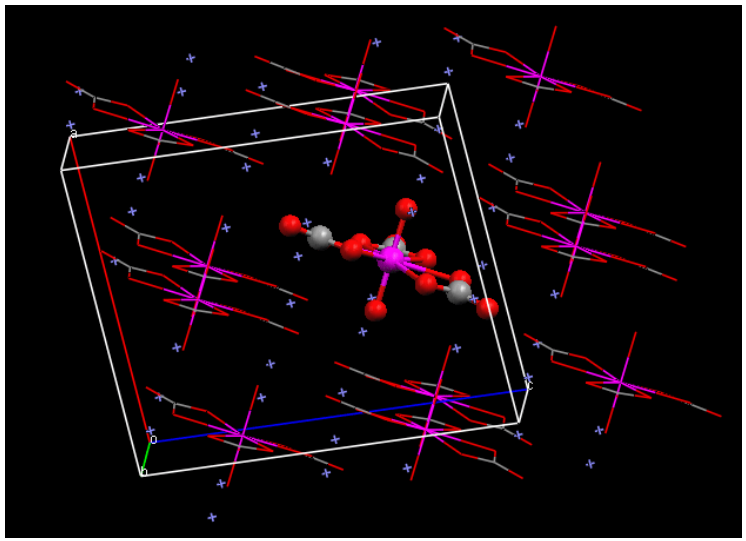

Crystal structure of $(NH_4)_4UO_2(CO_3)_3$

In this project computational chemistry is partnering with NMR experimentalists to develop a new tool for speciation of nuclear waste tanks at Hanford using the unique NMR signals of molecules.

Our calculated NMR property tensors predicted a very large chemical shift anisotropy for the ^{17}O NMR signal in uranyl carbonate crystals and a very broad NMR signal of around 1600 ppm.

Our predicted broad signal, which make the experimental measurements difficult, have been measured in experiments on uranyl nitrates and carbonates by Herman Cho, using the NMR facility in EMSL. A good agreement was found between the experimental and simulated spectrum.

Design of Anion Receptors

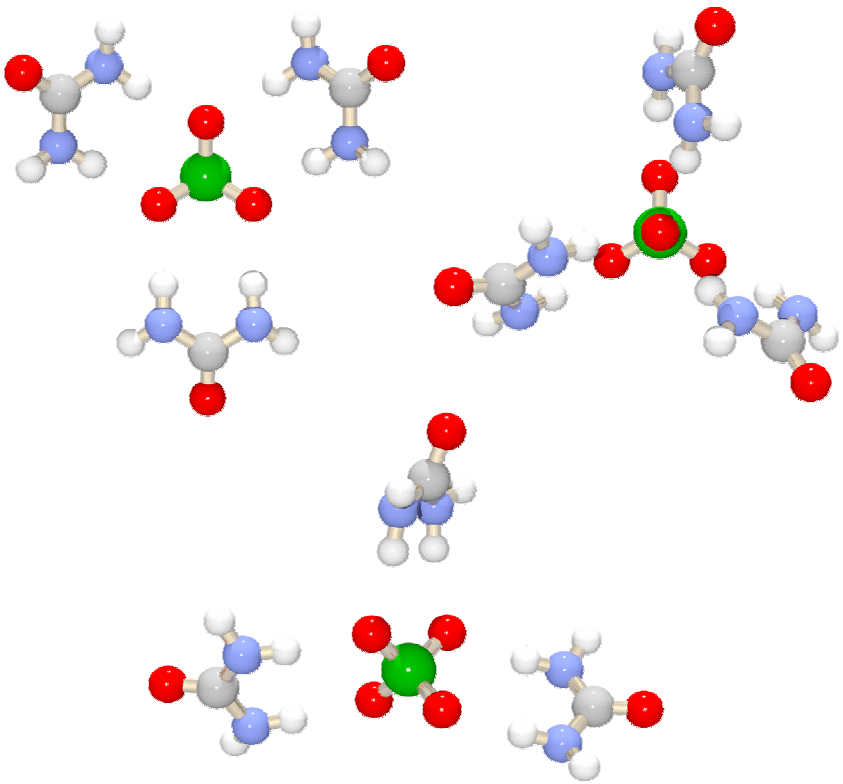

Optimized geometries for three configurations of a tris–urea perchlorate complex

We are using electronic structure calculations to examine complexes of urea, thiourea, and guanidinium chelates with a series of anions: chloride, nitrate, and perchlorate. These calculations have elucidated the structure of isolated chelates and their one–to–one anion complexes. The examination of the orientation and binding energies of multiple urea groups bound to a central anion is in progress. This knowledge is essential for the deliberate design of new chelating ligand architectures to enhance binding and selectivity over current ligands.

These new ligands are intended to facilitate waste cleanup projects, in collaboration with Bruce Moyer (ORNL)

Solvation of the Aqueous Electron

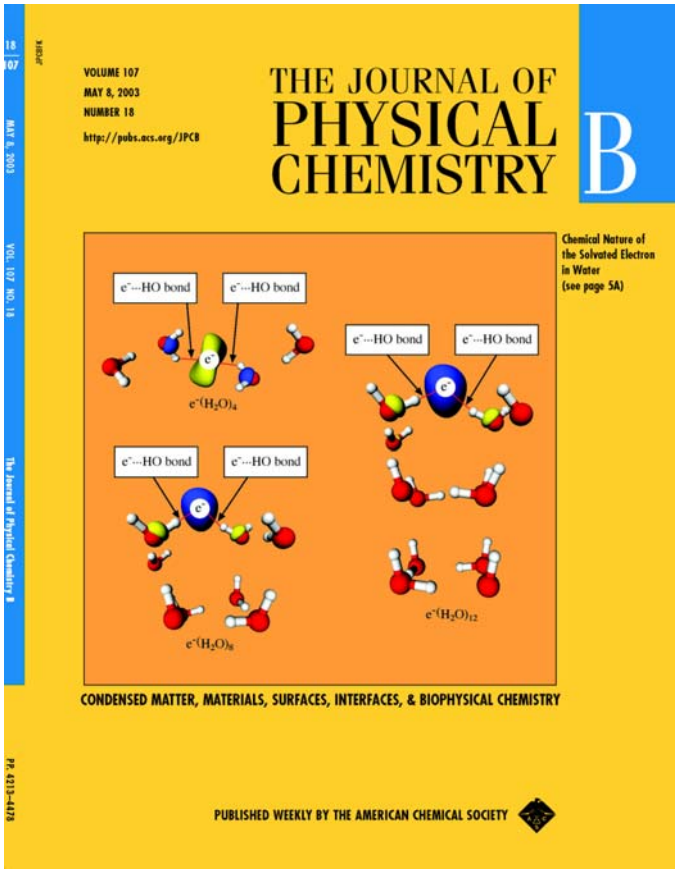

Featured on cover of J. Phys. Chem. B

The first first-principles solvation-included electronic structure study to energetically compare a variety of candidate structures of the hydrated electron and to determine its absolute hydration free energy, $\Delta G_{hyd}^{298}(e^-)$. The calculated results show that both the thermal motion and bulk solvent effects can qualitatively change the relative thermodynamic stability of different structures of the hydrated electron for a cluster of a given size, and that the most stable structure in solution is not necessarily the most stable one in the gas phase. For a given number of explicitly included solvent water molecules, the most stable structure in solution reveals a unique feature of the chemical nature of the solvated electron in water. The electron forms two strong electron-hydrogen bonds of the $e^-\cdots HO$ type with the hydrogen-bonded water cluster and two of the hydrogen-bonds in the neutral water cluster are broken. The absolute hydration free energy of the solvated electron in water has been calculated to be –35.5 kcal/mol by using a reliable computational protocol of first-principles solvation-included electronic structure calculations, and is in excellent agreement with a recently obtained experimental value of –34.6 kcal/mol. The predicted values for $\Delta G_{hyd}^{298}(e^-) + \Delta G_{hyd}^{298}(H^+)$ and $\Delta G_{hyd}^{298}(e^-) - \Delta G_{hyd}^{298}(HO^-)$ are in excellent agreement with the corresponding values derived from experimental data.

Understanding temperature and isotope effects in solvated $[TcO_4]^-$

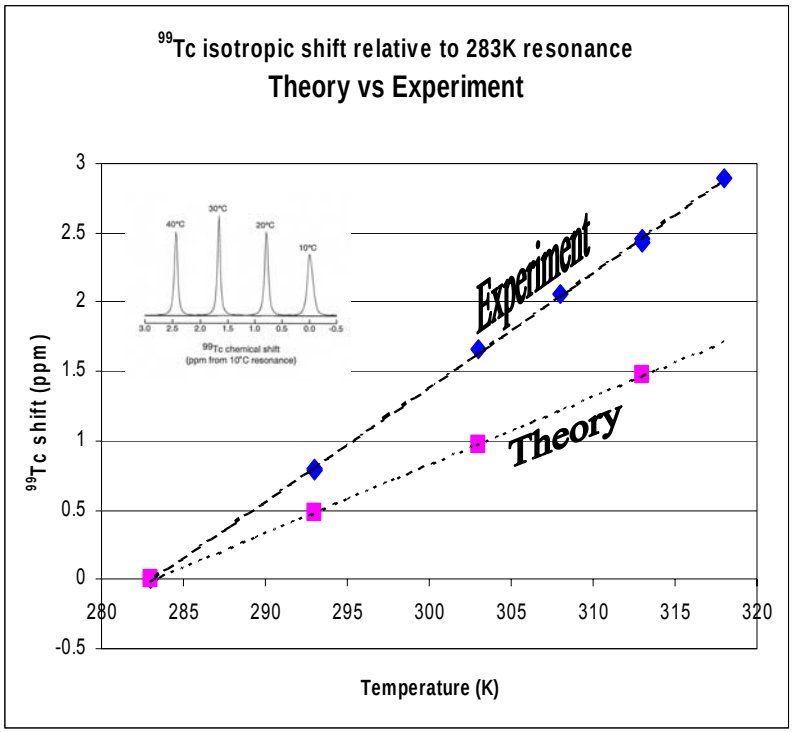

Comparison between experimental and calculated temperature dependence

Experiments on pertechnetate in solution have shown a temperature and isotope dependence of both ^{99}Tc chemical shift (CS) and the ^{99}Tc-^{17}O spin-spin (J) coupling.

To interpret the isotope and temperature dependence of the chemical shielding and spin-spin coupling we need to include the (anharmonic) vibrational, and rotational motion of the molecule in solution at a finite temperature.

Ab initio calculations were performed in order to obtain the vibrational averaged structure and chemical shift of pertechnetate in the solution.

Calculations are able to predict the experimentally observed trends.

DFT analysis of Uranyl – CCl_4 Interactions

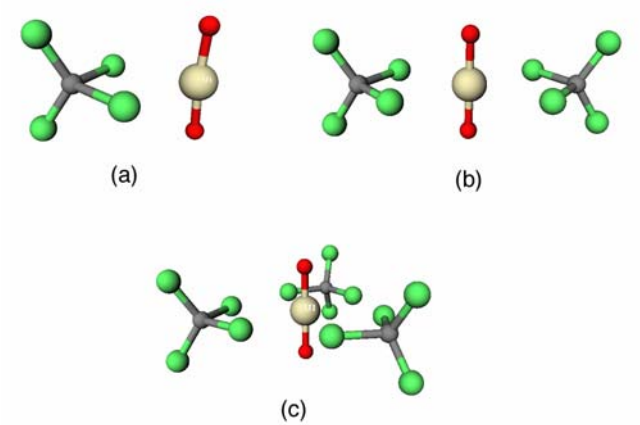

Optimized structures for $UO_2(CCl_4)_n$

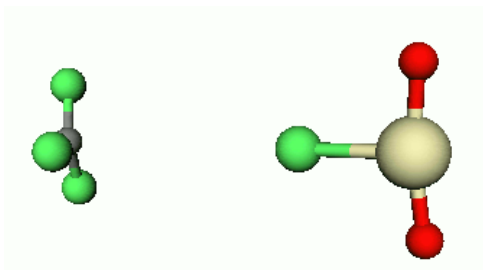

Dissociated structure for $UO_2(CCl_4)$

Understanding of the potential reactions of uranyl and carbon tetrachloride (CCl_4) is critical for the remediation of radioactive wastes at the Hanford site. Determination of solvent phase energetics will assist in the creation of reliable fate and transport models for uranyl species.

DFT frequency calculations on $[UO_2(CCl_4)]^{2+}$ give substantial imaginary vibrational frequencies, indicating instability in the system.
A possible dissociation reaction has been determined where one of the chlorides associates with uranyl and the CCl_3 molecule departs (see figure on the bottom). Examination of the reaction path, in gas phase and in the presence of water, reveals a very small dissociation barrier (approximately 2 kcal/mol). When more carbon tetrachlorides are added the complex becomes more stabe.

Actinide-Noble Gas Bonding

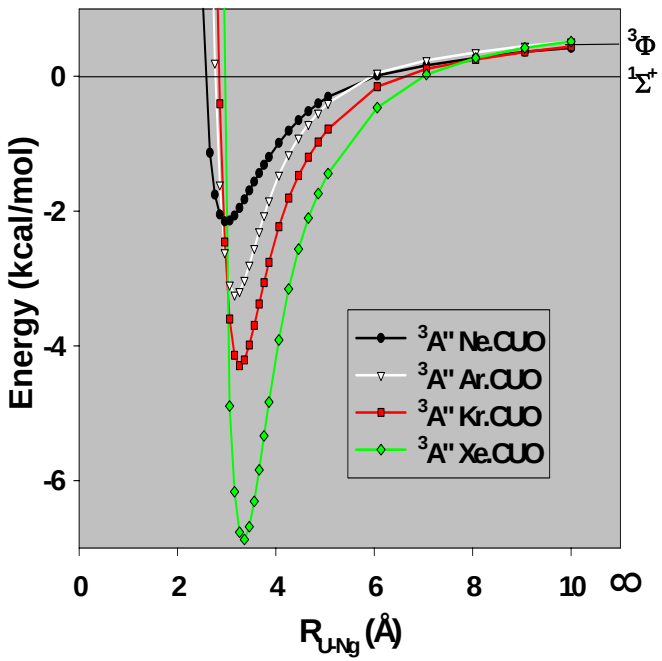

Energy Curves of CUO(Ng)
(Ng = Ne, Ar, Kr, Xe)

In collaboration with the Andrews group at the U. of Virginia we have performed systematic experimental and theoretical investigations on the $CUO(Ng)_x$ (Ng = Ne, Ar, Kr, Xe) complexes to further understand the geometries, energetics, vibrational properties, bonding between U and Ng atoms, and actinide noble-gas coordination chemistry. We find that

(1) The interaction between U and Ng atom increases when Ng changes from Ne to Xe (figure on the left)
(2) Relativistic spin-orbit coupling (SOC) effects will help to stabilize the triplet first excited state to bring it energetically close to the singlet ground state
(3) Without SOC, the triplet-singlet separation is 14.0 – 16.0 kcal/mol for CUO, and each CUO(Ng) at the CCSD(T) level, indicating multiple heavy Ng atoms are needed to reverse the ground state of CUO from singlet to triplet state

These results have been published in (a) Andrews, Liang, Li, Bursten, ***J. Am. Chem. Soc.*** **2003**, *125*, 3126-39. (b) Liang, Andrews, Li, Bursten ***Chem. Eur. J.*** **2003**, *9*, 4781-8. (c) Bursten, Drummond, Li, ***Faraday Discuss.*** **2003**, *124*, 1-24. (d) Andrews, Liang, Li, Bursten, ***New. J. Chem.*** in press.

Ionic hydration

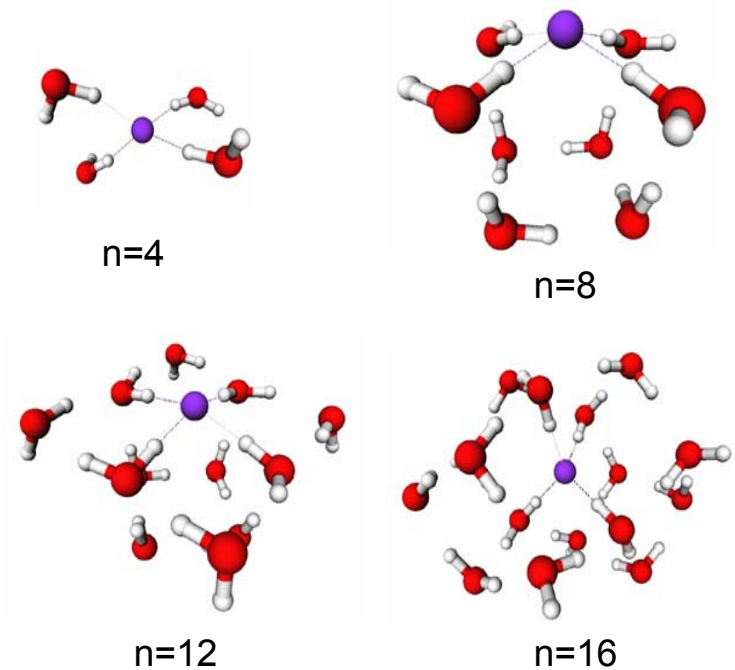

Most stable structure of $F^-(H_2O)_n$ in solution

A series of first-principles electronic structure calculations to determine the most stable structures of the $F^-(H_2O)_n$ clusters (n = 4, 8, 12, and 16) and to determine the hydration free energy of fluoride anion (F^-) were performed at the DFT and ab initio MO theory levels. The relative stability of the hydration structures changes from n = 8 to 12 to 16. The tetrahedrally coordinated fluoride anion hydration structure becomes more stable as compared to hydration structures with a pyramidal coordination, i.e., a surface ion cluster state. With increasing n, the fluoride anion will be internally solvated in large enough $F^-(H_2O)_n$ clusters. This provides insight into the transition from the hydration structure found in small gas phase hydrated anion clusters to the hydration structure observed in aqueous solution. The absolute hydration free energy of fluoride anion in aqueous solution, $\Delta G_{hyd}^{298}(F^-)$, is predicted by using a reliable computational protocol of first-principles solvation-included electronic structure calculations, the same approach recently used to calculate the absolute hydration free energy of H^+, OH^-, and the electron. The predicted $\Delta G_{hyd}^{298}(F^-)$ together with our previously calculated $\Delta G_{hyd}^{298}(H^+)$ determined by using the same computational protocol, gives $\Delta G_{hyd}^{298}(F^-) + \Delta G_{hyd}^{298}(H^+) = -366.7 \pm 0.7$ kcal/mol in excellent agreement with the value of –366.5 kcal/mol derived from the available experimental data.